

GA-ANN Prediction Model for Establishment of Langmuir Isotherm and characteristics study of Langmuir Isotherm constants

Satyaveer Singh¹, Annapurna Barouah²

UPES, Dehradun, UK-248007, India

Abstract:- Adsorption of gases on solid surface is very common phenomenon and naturally occurs in nature. Langmuir Isotherm is commonly used to describe the adsorption of gas on solid surface due to its very similar pattern depiction as derived from experimental data. A profound understanding of Langmuir Isotherm establishment and its dependency on different influencing parameters is very essential for prediction of sorption process of gas on solid surface. Langmuir Isotherm establishment depends on Langmuir constants, so very precise evaluation of Langmuir constants is essential for successful accurate establishment of Langmuir Isotherm.

In this paper dependency of Langmuir constants on coal quality parameters (moisture, volatile matter, fixed carbon, ash content and vitrinite reflectance) and temperature have been studied to predict Langmuir constants for establishment of Langmuir Isotherm for coal in a specified geological condition without going into tedious and time consuming experimental experiments. Genetic Algorithm (GA) and Artificial Neural Network (ANN) in combination have been used as a mathematical modelling tool for prediction Langmuir constants for sorption study. This study reveal that Langmuir Volume Constant (V_L) depends on properties of sorbent only while Langmuir Pressure constant (P_L) depends on properties of sorbent and physical condition of sorption system. As the coal quality parameters changes for every point, so this prediction model would be very useful in insitu gas estimation by real time modelling of coal reservoir.

Keywords: Sorption, Langmuir Isotherm, Langmuir constants, Genetic Algorithm (GA), Artificial Neural Network (ANN)

1. Introduction

Methane is the cleanest form of all burning fossil fuel having heating value of approximately 8500 KCal/kg [1]. Methane is naturally occurring in coal bed and natural gas reservoir. Methane associated with coal bed is also called as Coal Bed Methane (CBM). Coal bed methane is generated during coalification process, some amount of generated gas adsorbed into coal matrix itself at higher pressure while some amount of generated gas migrated and get entrapped into a distant located natural gas reservoir [2]. Coal seam serve as a source and reservoir rock for CBM, while in conventional gas reservoirs the source and reservoir rocks are different [3]. Generated methane gas retention in coal bed is depends on sorption capacity of coal and geological condition [4]. Coal system is complicated matrix-fracture system. The micropores in coal matrix have very large amount of area to store the gas in adsorbed state and bind with the surface free energy of coal [5]. CBM stored in coal seam is mainly in adsorbed state into micropores of coal matrix. Sorption of gas into coal matrix depends on coal quality, coal rank, macerals content, cleats in coal matrix, geological burial pressure and temperature[6] [7] [8][9][10]. Dependency of Langmuir constants on temperature have been studied by different researchers [11] [12] [13].

Diffusion rate of gas is estimated by Diffusion coefficient. Diffusion coefficient of gas is also depend on adsorption capacity of coal. Diffusion coefficient of CBM reservoir can be estimated on the basis of adsorption amount [14]. Due low permeability and insitu stress of CBM reservoir, its recovery is low (around 50%) in normal case. CBM hydraulic fracturing and insertion of inert gas into coal matrix are some stimulation techniques to increase the CBM recovery by improving diffusion rate [15].

Langmuir Isotherm is commonly used Isotherm in industry to estimate the sorption of gas in coal matrix due to its simplicity and near to most accurate estimation [11] [13]. It has been found a very good resemble of Langmuir Equation with experimental data of CH₄ gas adsorption into coal matrix [16]. The adsorption theory was developed in 1918 with a specific assumption, “A gas molecule always adsorbed at single adsorption site and it does not affect the neighboring site. The gas molecules adsorption on open surface with lack of gas access to sites and the sites are indistinguishable by the gas molecules.” [17].

On the basis of above considered assumption Langmuir Isotherm equation is derived and given below:

$$V = V_L * P / (P + P_L)$$

Where,

V=Volume of gas adsorbed per unit weight of solid at pressure P

V_L= Langmuir Volume constant (Maximum amount of gas adsorbed per unit weight of solid)

P_L=Langmuir Pressure constant (Pressure at which half of the maximum possible gas adsorbed)

Some of the researchers have tried to establish the prediction equation to predict the Langmuir constants for insitu gas estimation on the basis of coal quality parameters and geological conditions. The Langmuir Rank Equation [19], Jian Shen established prediction equation [20], and AK Verma prediction model [12] are some of the work done for prediction of Langmuir constants. Kim’s empirical equation was given for direct estimation of insitu gas on the basis of proximate analysis [21]. The detail of above mentioned prediction equations and model are given in Table 1.

Table 1 (Adsorption Prediction Model)

Name of predictor equation/ Model	Equations	Remark
Langmuir Rank Equation [19]	$V = V_L * P / (P + P_L)$ $\log(V_L) = k_1 * \log(FC/VM) + k_2$ $\log(P_L) = k_3 * \log(FC/VM) + k_4$ K_i is temperature dependent	Only FC _{daf} , VM _{daf} and temperature are considered to evaluate adsorption. The direct effect of Ash content, Moisture and Maceral effects are not considered.
Jian Shen established equation [20]	$V = V_L * P / (P + P_L)$ $V_L = (17.65 * R_o + 10.97) * e^{(-0.0098T)}$ $P_L = 4.44 * R_o^2 - 17.32 * R_o + 19.81$	Only Maceral effects and temperature dependency are considered in prediction model but other influencing coal parameters not considered.
Kim’s Equation [21]	$G_c = (1 - w - a) V_w * (k_0 * P^{n_0} - bT) / V_d$ $V_w, V_d, K_0 \& n_0$ are kims constant	All Proximate Parameters and temperature are considered in prediction model. Only Maceral effects are not considered, but this prediction model was established on the basis of regression analysis not with soft robust computing technique.

Where,

V =Volume of gas adsorbed per unit weight of solid at pressure P

V_L = Langmuir Volume constant

P_L =Langmuir Pressure constant

FC = Fixed Carbon % in proximate analysis

VM = Volatile Matter % in proximate analysis

R_o = Maximum Vitrinite Reflectance

T = Temperature

G_c = Insitu Volume of gas adsorbed per unit weight of coal

A comparison for the efficacy of all the above mentioned prediction models with our proposed prediction model have been done and shown in Table 3.

Genetic Algorithm (GA)

Genetic Algorithm (GA) is very powerful optimization tool and provide better optimization solution of the problem than conventional one. Genetic algorithm is based on the principle of natural genetics and natural selection rule [22]. GA generates different population sets for getting solution of the problems with optimisation technique. A fitness function evaluates the weightage of each solution and contribution to the next level of offspring decided accordingly. A crossover mechanism among the parents like gene transfer in sexual reproduction, the algorithm creates a new population for GA solutions [23]. The following steps are mainly used in Genetic Algorithm (GA)

- Definition of objective function
- Encoding of fitness function
- Reproduction
- Cross over
- Mutation

Artificial Neural Network (ANN)

Artificial neural network (ANN) is supervised learning technique and inspired by biological nervous system [24]. A network is formed on the basis of transfer function. Network is trained to perform a particular function with mathematical connection (weights and biases) between elements. The formed network with specific transfer function is used to transfer the input data to neuron layer. The elements are connected with some weights and biases to attain the specified goal. This trained network is used for prediction purpose.

Feed forward back propagation is used in this work. The feed forward back-propagation neural network (BPNN), the received inputs are forwarded through neuron to the entire next layer with connected weight and biases to obtain the outputs and these weight and biases are modified in next step on the basis of performance of error function [25]. These weights and biases are modified in each training steps according to generated rule. A sigmoid layer and a linear output layer of transfer functions are capable of approximating any function in BPNN [26].

Combined Genetic Algorithm and Artificial Neural Network (GA-ANN)

Genetic Algorithm (GA) and Artificial Neural Network (ANN) are very powerful optimizing and learning techniques for problem solving, but both have its own strength and weakness [27]. By combining Genetic Algorithms with Neural Networks (GA-NN) may provide a better result by overcoming its weakness. Nature also represent very successful implementation of GA-ANN in natural process of progression. Success of any species depends on its natural evolution as well as its own learning for improvement [27].

With small data set ANN prediction model may stuck into network over fitting during network training which may provide very erroneous result. For network generalization Bayesian regularization, early stopping or very large data set is required for establishment of correct ANN prediction model. With use of Bayesian regularization

and early stopping for small data set, network over fitting problem may be avoided but this trained network provide very error in prediction due to diverged training. GA provide reasonable output even with small data set. GA may be used to increase data set reasonably for better result by ANN. Combining the GA with ANN, which is termed here as GA-ANN is very useful in modelling with small data set. A supportive approach of combining of the GA and ANN has been used in this study for preprocessing of data by GA and preprocessed data use in ANN for better result.

2. Objectives

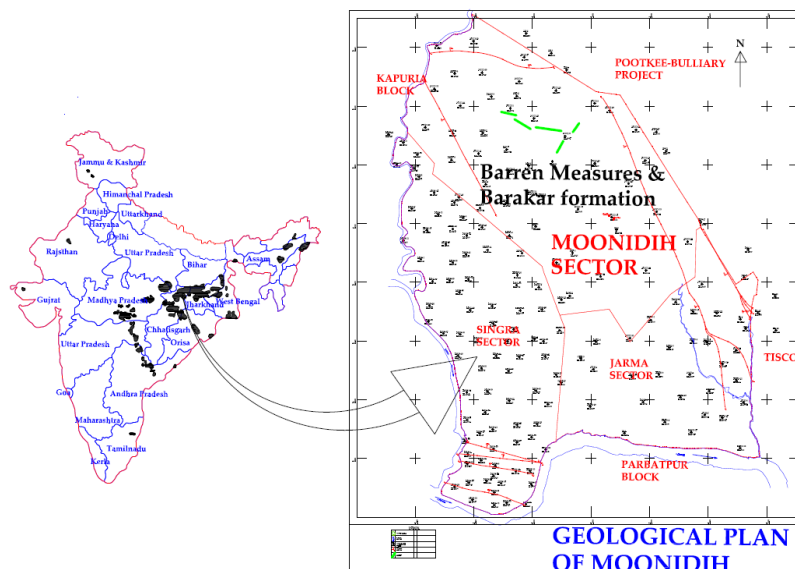
Estimation of Langmuir constants (V_L & P_L) is done by experimental adsorption studies of gas on coal sample in specially designed adsorption isotherm bath tub attached with gas chromatograph. The adsorbed volume of gas into coal sample at different pressures and constant temperature is to be measured by experimental adsorption studies for establishment of Langmuir isotherm [18]. As the coal quality parameters may vary from point to point of coal reservoir. So it is very difficult to do the experiment for all coal to evaluate Langmuir constants.

A prediction model based on GA-ANN soft computing tool has been established to assess the Langmuir constants. On the basis of assessed Langmuir constants, Langmuir isotherm would be established to estimate the sorption of gas into coal matrix. The characteristic study of Langmuir constants (V_L & P_L) depending on different parameters have also been studied in this paper for better understanding of sorption process.

3. Methods

The data set considered in this study for prediction modelling are taken from experimental data set and previous various published studies. 80 Nos. of data set of worldwide located coal samples from experimentally evaluated data of Singrauli Coalfield, India and previous available different worldwide literatures have been considered. The collected data sets have been converted into a standard SI unit and used for modelling of GA prediction model & GA-ANN prediction model. The referential detail of considered data set are given in Annexure-I [9].

Coal from Moonidih Mine has been used for testing of established prediction GA model & GA-ANN prediction model. CBM Project of Moonidih is located in the central part of the Jharia coalfield in Dhanbad district of Jharkhand, India. It is included in the Survey of India Toposheet No. 73 I/5 & I/6 (R.F 1:50,000). Jharia coalfield is completely covered by the Barren Measure Formation rocks (Middle Permian), overlying Barakar Formation (Lower Permian). Total 51 Nos. of coal seams including splits and local seams/coal bands occur in the Barakar formation of Moonidih, however, 18 of them are persistent. Seam No. V, VI & VII are thick and prominent seam for CBM.



Langmuir constants for coal sample collected from XV-Top seam of Monidih Mine has been experimentally evaluated by Laboratory of CMPDI, Ranchi. The measured value of coal quality parameters and Langmuir constants from experimental data has been used to validate the efficacy of developed GA-ANN prediction model.

GA Model

GA model developed here uses important parameters on which Langmuir constants depends. The GA prediction model has been developed by using coal quality parameters (moisture, volatile matter, fixed carbon, ash content and vitrinite reflectance) and temperature as a input parameters and Langmuir constants (P_L & V_L) as output parameters. A fitness function has been encoded in MATLAB for prediction of Langmuir constants (P_L & V_L) with coal quality parameters and temperature alongwith corresponding prediction constants (a_i & b_i). GA optimisation has been used for minimisation of objective function and estimation of prediction constants (a_i & b_i) [9].

$$Z_1 = \sum |P_{Loi} - P_{Lci}| \text{ and } Z_2 = \sum |V_{Loi} - V_{Lci}|$$

Where,

P_{Lo} = Observed value of P_L in (MPa)

P_{Lp} = Predicted value of P_L in (MPa)

V_{Lo} = Observed value of V_L in (Sm^3/t)

V_{Lp} = Predicted value of V_L in (Sm^3/t)

The following parameters has been considered to establish GA prediction model:

- 13 Nos. of variables as prediction constant in fitness function
- Rank based fitness scaling function
- Stochastic Uniform selection function
- Gaussian Mutation function
- Heuristic Crossover function

The 80 No. of data set has been taken from experimental studies of coal samples from Main Basin of Singrauli coalfield, India and worldwide earlier published data set (Annexure-I) [9]. The parameters of the above referenced published data set has been utilized by GA tool to minimize the objective function for evaluation of Prediction constants (a_i & b_i). GA modelling plot for estimation of prediction constants in Langmuir Pressure Constant (P_L) and Langmuir Volume Constant (V_L) are shown in Fig. 1 & Fig. 2 respectively.

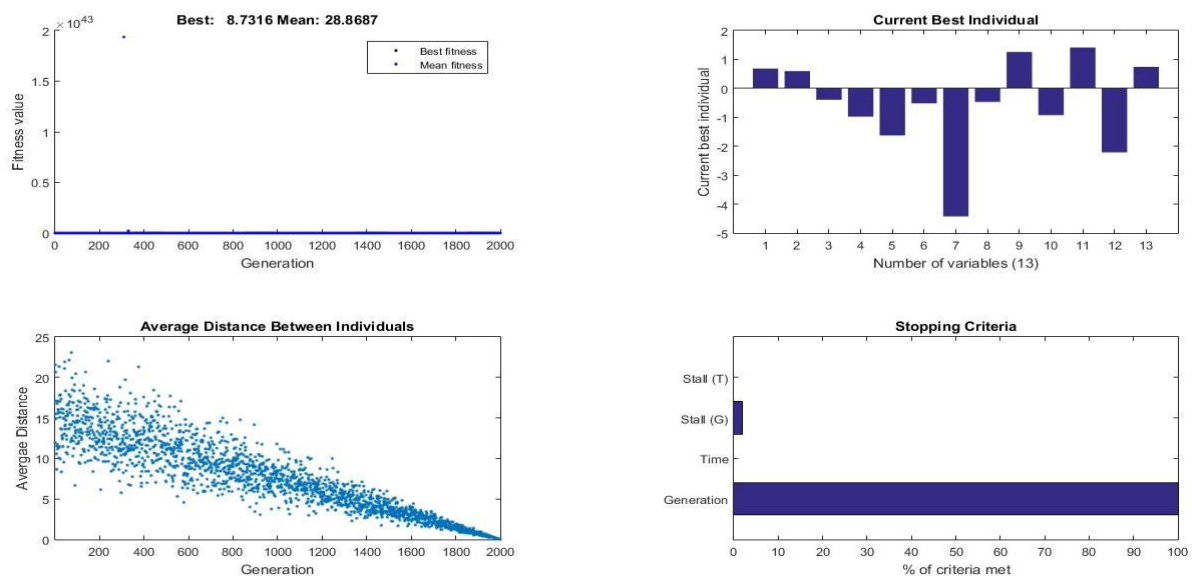


Fig. 1 (GA modelling Graph for Langmuir Pressure Constant P_L)

- (A) Fitness value of objective function Vs Generation of offspring (B) Best fitted value of individual variables Vs Variables (C) Convergence Vs Generation of offspring (D) Stopping Criteria to overcome defined limit for GA process

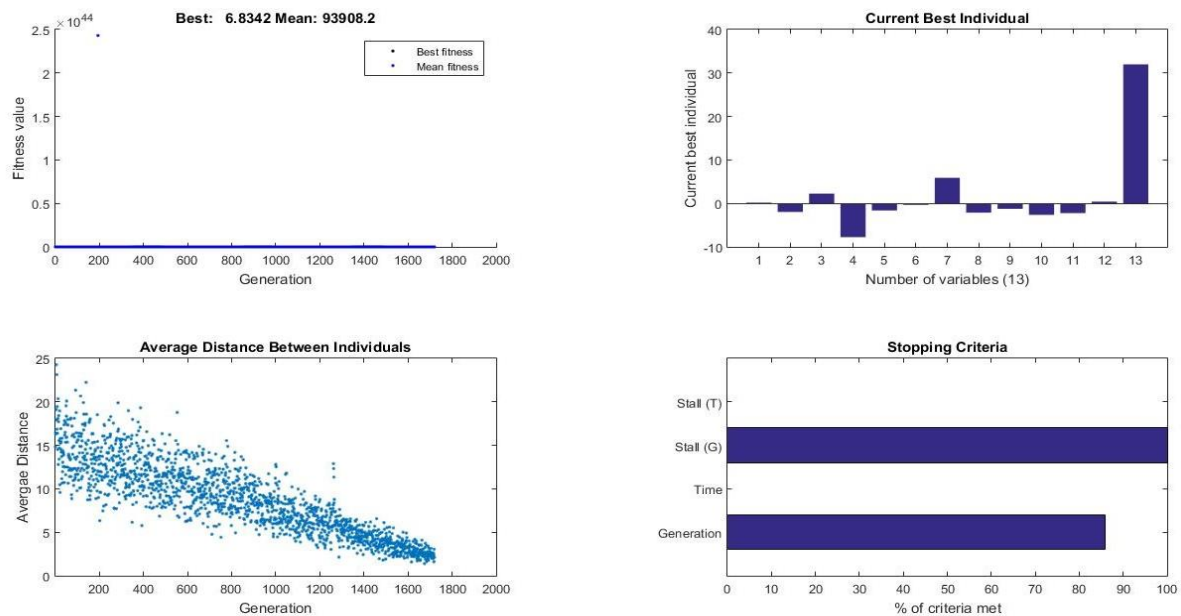


Fig. 2 (GA modelling Graph for Langmuir Volume Constant V_L)

(A) Fitness value of objective function Vs Generation of offspring (B) Best fitted value of individual variables Vs Variables
(C) Convergence Vs Generation of offspring (D) Stopping Criteria to overcome defined limit for GA process.

The full convergence of generation in GA model are shown in above plots depict the best evaluation of the Prediction constants in the considered Objective function with possible minimum deviation (error) in prediction modelling.

GA-ANN Model

The 80 No. of experimental data set (Annexure-I) has been considered in this study [9]. This is small data set for neural network modelling with 6 Nos. of input parameters. So, A GA model has been developed with 80 experimental data set. 460 Nos. of rationalized random data has been used as input data to generate corresponding output of the data by GA model. These 80 experimental data and 460 GA predicted data set has been used for ANN modelling. This GA-ANN developed model is a basically ANN model, which is modeled based on 80 experimental data set and 460 GA predicted data set. Detailed Network architecture for GA-ANN is shown in Fig. 3.

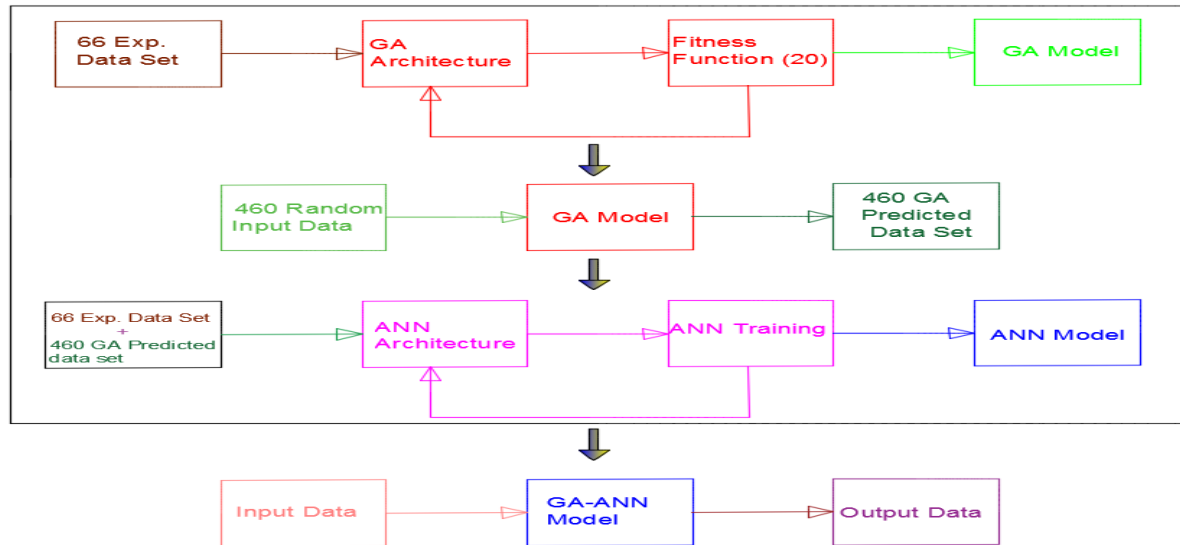


Fig. 3 (GA-ANN Network Architecture)

Feed forward back propagation network (BPNN) is adopted for the problem. A network of three layers has been set for the problem with 6 Nos. of input variables (Moisture (M), Volatile Matter (VM), Fixed Caron (FC), Ash (A), Vitritine Reflectance (Ro) and Temperature (T)) and 2 output variables (Langmuir Pressure Constant (P_L) & Langmuir Volume Constant (V_L)). The ANN network architecture consist 6 input and 2 output alongwith network of 18 neurons in input layer and 12 neurons in first intermediate layer to develop prediction model. Transfer functions are set 'tansig', 'logsig' and 'purelin' for input layer, first intermediate layer and output layer correspondingly. The defined network has been trained with 'trainbr' function. Bayesian regularization function 'trainbr' has been used to avoid over fitting. Neural Network architecture showing neurons and ANN defined layer-wise network are shown in Fig. 4a and Fig 4b respectively.

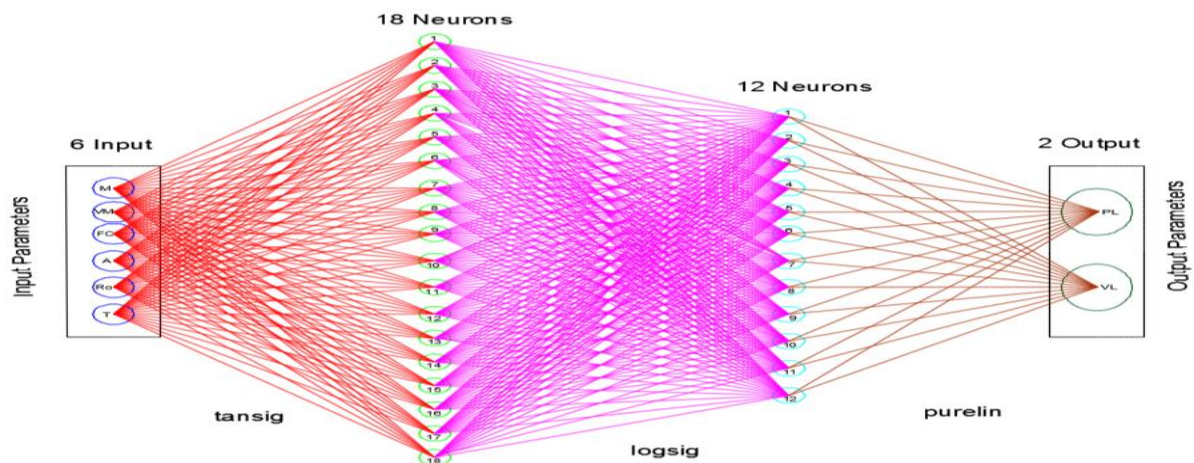


Fig. 4a (ANN Model Network Architecture)

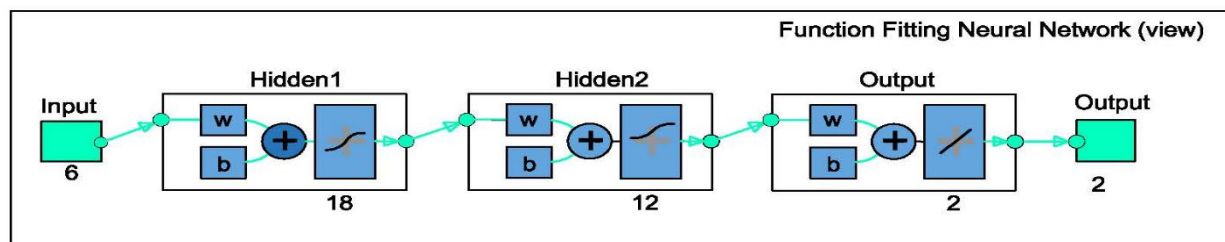


Fig. 4b (ANN defined layer-wise Network with transfer function)

70% of input data has been used for training, 15% of input data has been used for validation and 15% of input data has been used for testing. Training and Testing performance of network is given in Fig. 4c.

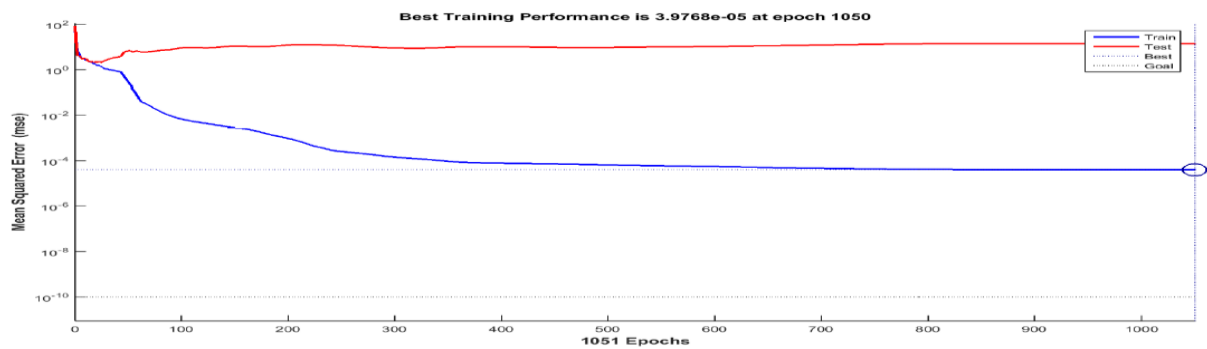


Fig. 4c (Mean Square Error Vs ANN iteration showing ANN Training & Testing Performance)

The regression analysis for training and testing of ANN model is given in Fig. 5.

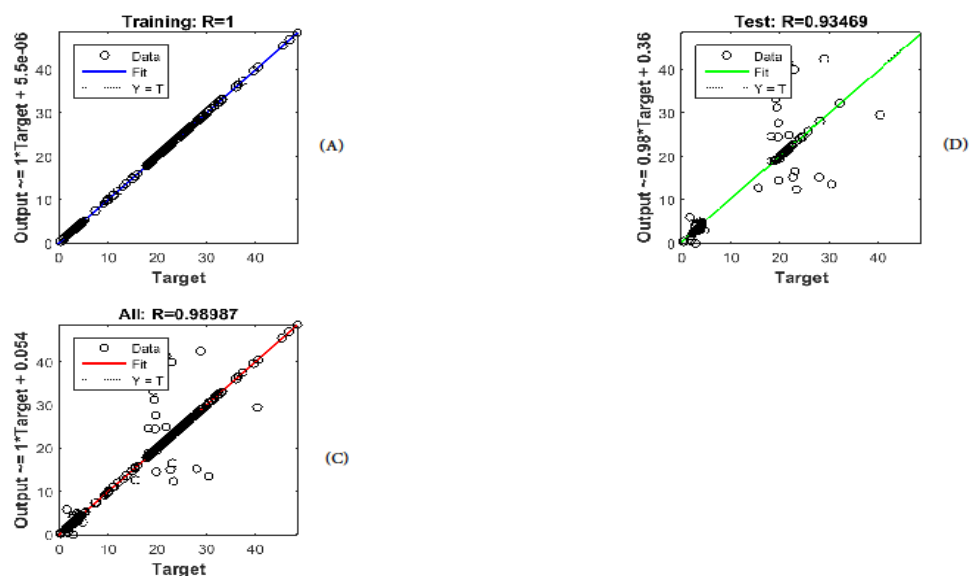


Fig. 5 (Regression Analysis of ANN model Training & Testing)

(A) Regression Analysis for Training data (B) Regression Analysis for Testing data (C) Regression Analysis for total data set

The regression analysis of ANN model shows that regression coefficient for training data set is 1 while in testing data set regression coefficient is 0.93 and for overall data set regression coefficient is 0.98. So prediction model efficient and has sufficient accuracy.

4. Results

GA Prediction Model

The fitness function used in GA model is absolute percentage error function derived from experimental data and predicted data of Langmuir Pressure constant (P_L) and Langmuir Volume constant (V_L). Langmuir constants (P_L and V_L) may be expressed as a linear polynomial function of coal quality parameters and temperature along with 13 Nos. of corresponding prediction constants.

$$P_L = a_1 * M^{a_2} + a_3 * VM^{a_4} + a_5 * FC^{a_6} + a_7 * A^{a_8} + a_9 * R_o^{a_{10}} + a_{11} * T^{a_{12}} + a_{13};$$

$$V_L = b_1 * M^{b_2} + b_3 * VM^{b_4} + b_5 * FC^{b_6} + b_7 * A^{b_8} + b_9 * R_o^{b_{10}} + b_{11} * T^{b_{12}} + b_{13};$$

Where

P_L = Langmuir Pressure Constant (MPa)

V_L = Langmuir Volume Constant (Sm^3/t) dry ash free basis (daf)

M = Moisture (%) air dry basis (ad)

VM = Volatile Matter (%) air dry basis (ad)

FC = Fixed Carbon (%) air dry basis (ad)

R_o = Vitrinite Reflectance

T = Temperature (OC)

a_i = Prediction Constants for P_L

b_i = Prediction Constants for V_L

Output Parameters

Input Parameters

The value of 13 Nos. of prediction constant used in GA prediction model for Langmuir constant derived by GA tool have been enlisted in Table 2.

Table 2. (Prediction Constants (a_i & b_i) for P_L & V_L)

Prediction Constant (a_i) for Langmuir Pressure Constant (P_L)	a_1	a_2	a_3	a_4	a_5	a_6	a_7	a_8	a_9	a_{10}	a_{11}	a_{12}	a_{13}
	-0.08	1.81	5.80	-0.21	16.76	-0.08	9.66	0.17	3.05	-0.09	0.10	0.09	0.36
Prediction Constant (b_i) for Langmuir Volume Constant (V_L)	b_1	b_2	b_3	b_4	b_5	b_6	b_7	b_8	b_9	b_{10}	b_{11}	b_{12}	b_{13}
	-0.13	2.53	7.20	-0.25	23.18	-0.14	-1.16	0.10	-0.10	-0.20	-0.09	0.09	2.62

The average percentage error in prediction and experimental data set used for testing of GA model are 10.64% and 7.44% for Langmuir Pressure constant (P_L) and Langmuir Volume constant (V_L) respectively. The above GA model uses all possible influencing parameters as input parameters, which increases the reliability and efficacy of the prediction model.

GA-ANN Prediction Model

The 80 experimental data and 460 GA predicted data set has been used for ANN modelling. 15% of input data has been used for testing of the ANN model. The percentage error during testing of GA-ANN model in the process of ANN modeling are 4.19% and 2.57% for Langmuir Pressure constant (P_L) and Langmuir Volume constant (V_L) respectively.

The detail of 6 Nos. input parameters and 2 Nos. output parameters used in GA-ANN model are given below:

P_L =Langmuir Pressure Constant (MPa)	Output Parameters
V_L = Langmuir Volume Constant (Sm^3/t) dry ash free basis (daf)	
M= Moisture (%) air dry basis (ad)	Input Parameters
VM = Volatile Matter (%) air dry basis (ad)	
FC= Fixed Carbon (%) air dry basis (ad)	
R_o =Vitrinite Reflectance	
T=Temperature ($^{\circ}\text{C}$)	

A comparison of prediction model has been done among established GA prediction model & GA-ANN prediction model and Langmuir Rank Equation prediction model & Jian Sen et al, 2015 prediction model suggested by different researchers. 30 Nos. of experimental data set collected from worldwide published literature has been used for comparison of these prediction models on the basis of absolute percentage error in predicted values and measured values. All comparisons have been enlisted in Table 3.

A bar chart diagram of average absolute percentage error (%) in prediction of 30 Nos. of data set by different prediction models has been shown in Fig. 6. The average absolute percentage error (%) in prediction of Langmuir Pressure constant (P_L) are 8.95%, 5.26%, 161.73% & 529.13% and Langmuir Volume constant (V_L) are 6.77%, 2.35%, 19.91% & 91.91% by GA model & GA-ANN model and Langmuir Rank Equation prediction model & Jian Sen et al, 2015 prediction model respectively. This shows that the developed prediction model using the soft computing tool in this study have better efficacy than other earlier developed prediction model by different reserchers. Soft computing tools is able to incorporate the impact of all the possible influencing parameters as input and which make the developed model more robust and reliable with greater accuracy in prediction.

Table 3 (Absolute % Error in prediction of Different Prediction Model)

Particulars		Experimental Data						GA Model			GA-ANN Model				Langmuir Rank Equation				Jian Sen et al., 2015																																																																																																																																																																																																																																																																																																																																																																																																																																																																																																																																																																																																																																																																																																																																																																																																																																																																																																																																																																																																																																																																																																																																																																																								
		Proximate Analysis (ad)			Temperature (°C)	Measured Value		Predicted Value		Error (%)	Predicted Value		Error (%)	Predicted Value		Error (%)	Predicted Value		Error (%)																																																																																																																																																																																																																																																																																																																																																																																																																																																																																																																																																																																																																																																																																																																																																																																																																																																																																																																																																																																																																																																																																																																																																																																								
Literature Reference	Sample Location	Moisture (%)	Volatile (%)	Fixed Carbon (%)		Ash (%)	R _{max} (%)	Langmuir Pressure Constant (P _L) (Mpa)	Langmuir Volume Constant (V _L) (sm ³ /t) (ad)		Langmuir (P _L) (Mpa)	Langmuir (V _L) (sm ³ /t) (ad)		Langmuir (P _L) (Mpa)	Langmuir (V _L) (sm ³ /t) (ad)		Langmuir (P _L) (Mpa)	Langmuir (V _L) (sm ³ /t) (ad)		Langmuir (P _L) (Mpa)	Langmuir (V _L) (sm ³ /t) (ad)	Langmuir (P _L) (Mpa)	Langmuir (V _L) (sm ³ /t) (ad)	Langmuir (P _L) (Mpa)	Langmuir (V _L) (sm ³ /t) (ad)	Predicted Value	Error (%)																																																																																																																																																																																																																																																																																																																																																																																																																																																																																																																																																																																																																																																																																																																																																																																																																																																																																																																																																																																																																																																																																																																																																																																

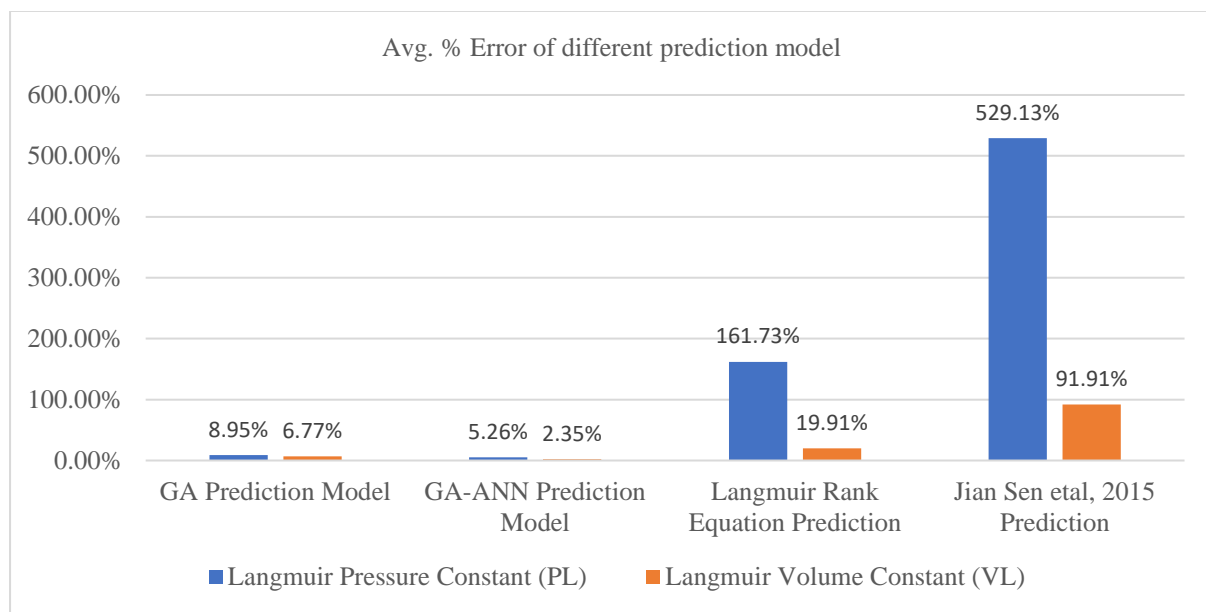


Fig. 6 (Avg. % Error in Prediction of Langmuir Pressure Constant (P_L) & Langmuir Volume Constant (V_L))

It is obvious from the Table 3 and Fig. 6 that avg. % error of prediction model is lowest for GA-ANN prediction model. The GA prediction model has slightly greater % error than the GA-ANN model but have significantly lesser than other researcher prediction model. The GA-ANN model can only be used in specific computer environment and observation of dependency of variable can't be done directly, while GA model provide a polynomial equation which can be utilized easily and dependency of variable can be observed directly. So both GA and GA-ANN model has its own pros and cons. So, developed GA & GA-ANN Prediction model can be used for prediction of Langmuir constant with greater accuracy and without time consuming.

Testing of Developed Prediction Models (GA & GA-ANN) with Experimental Data

Coal Sample collected from XV-Top seam of Monidih Mine has been experimentally tested for proximate analysis and Adsorption behavior of CH₄ gas at different temperatures. Coal quality Parameters (air dry basis) of coal sample based on the proximate analysis and Langmuir Constants estimated by CH₄ adsorption study on coal sample at different temperatures vis-a-vis Predicted by GA & GA-ANN prediction model are given in Table 4.

Table 4 (Coal Quality Parameters & Langmuir Constants)

Sample Location	Proximate Analysis				$R_{o,max}$ (%)	Temperature (°C)	Langmuir constants (Measured)		Langmuir constants (GA Predicted)		Absolute Error (%) (Measured and GA Predicted)		Langmuir constants (GA-ANN Predicted)		Absolute Error (%) (Measured and GA-ANN Predicted)	
	Moisture (%) (ad)	Volatile Matter (%) (ad)	Fixed Carbon (%) (ad)	Ash (%) (ad)			P_L (MPa)	V_L (sm ³) (daf)	P_L (MPa)	V_L (sm ³) (daf)	P_L (MPa)	V_L (sm ³) (daf)	P_L (MPa)	V_L (sm ³) (daf)	P_L (MPa)	V_L (sm ³) (daf)
XV-Top, Monidih Mine	3.6	23.2	59.6	13.6	1.1	30	2.56	21.19	2.37	22.19	7.61	4.70	2.478	22.13	3.20	4.44
	3.6	23.2	59.6	13.6	1.1	40	2.97	21.1	2.54	22.18	14.33	5.14	2.627	22.1	11.55	4.74
	3.6	23.2	59.6	13.6	1.1	50	2.98	21.05	2.69	22.18	9.75	5.38	2.783	22.08	6.61	4.89
	3.6	23.2	59.6	13.6	1.1	60	3.01	21.05	2.81	22.18	6.57	5.37	3.152	22.06	4.72	4.80
	3.6	23.2	59.6	13.6	1.1	70	3.25	21.01	2.92	22.18	10.19	5.57	3.2	22.05	1.54	4.95
Average Absolute Error (%)											9.69	5.23			5.52	4.76

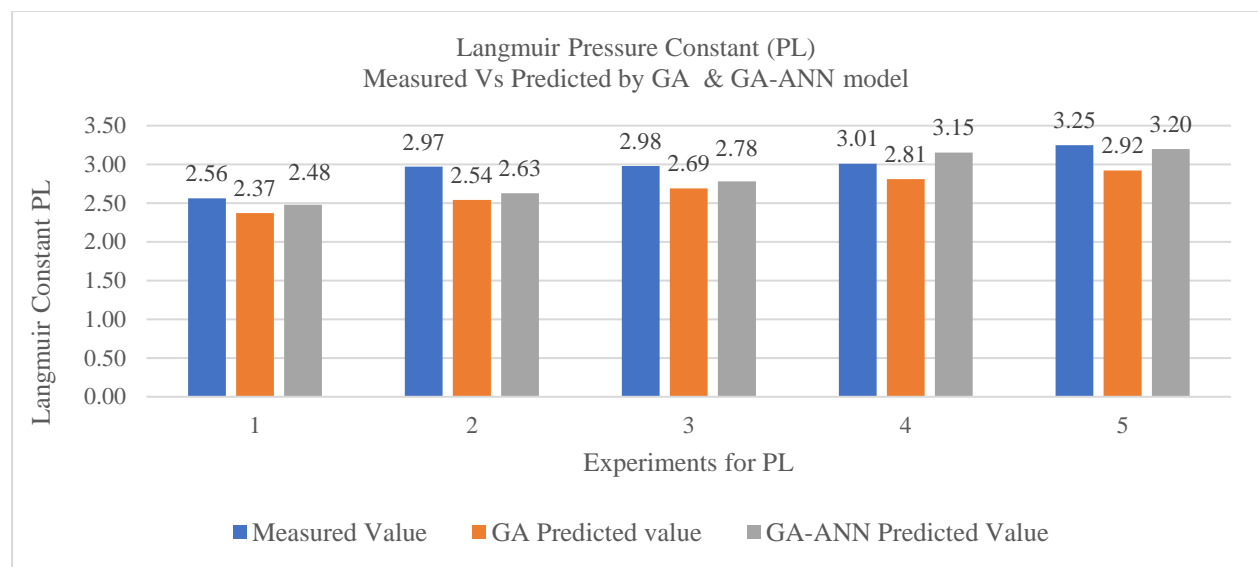


Fig. 7a (Langmuir Pressure constant (P_L))
(Measured value vis a vis Predicted value by GA & GA-ANN model)

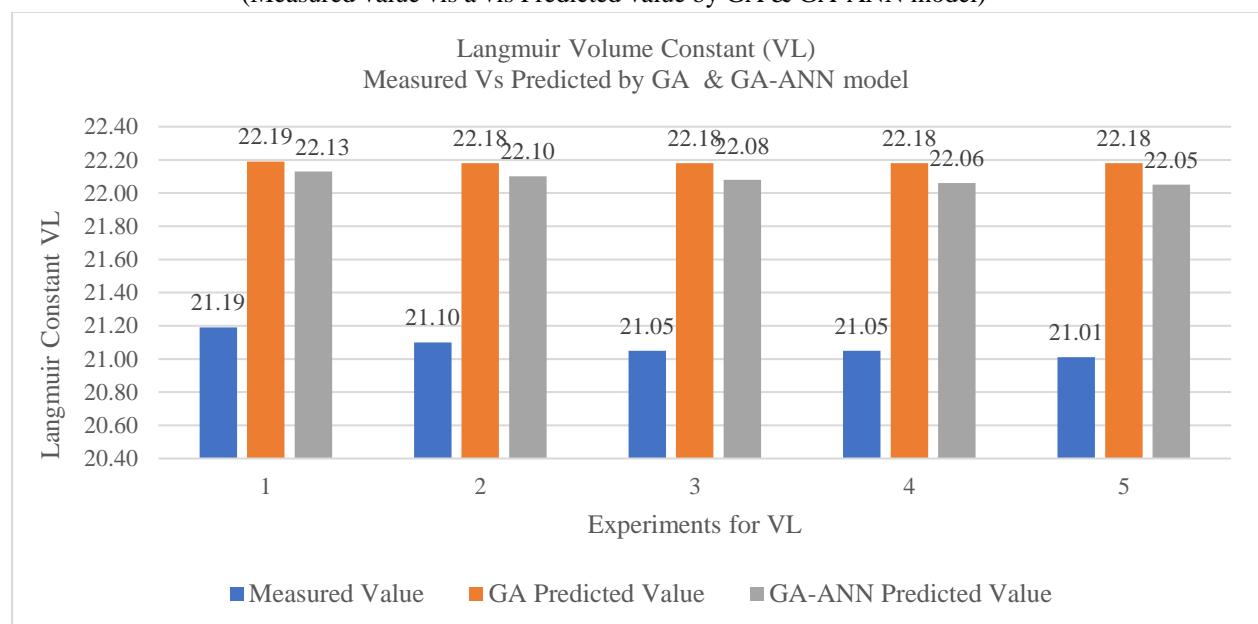


Fig. 7b (Langmuir Volume constant (V_L))
(Measured value vis a vis Predicted value by GA & GA-ANN model)

It is illustrated by Table 4 and Fig. 7a & 7b that established both Prediction model (GA Prediction model and GA-ANN Prediction) are able to predict Langmuir constants quite accurately, while GA-ANN Prediction model is more robust and predict more accurately.

Study of Langmuir Constants

The developed both GA & GA-ANN prediction model have sufficient accuracy in prediction of Langmuir constants. These have been used for correlation study of Langmuir constants with various influencing parameters. The value of Langmuir constants have been predicted by both GA & GA-ANN model with varying value of only one influencing variable keeping other influencing variables constant. So the impact of change in one influencing variable on Langmuir constants can be accessed by these prediction models. The graph between Langmuir Constants (P_L & V_L) Vs different variables have been plotted and best curve fitting equation alongwith regression coefficient R^2 have been shown on the graph for correlation study.

Study of Langmuir Pressure Constant (P_L) Vs Moisture (M_{ad} %), Volatile Matter (VM_{ad} %), Ash (A_{ad} %), Vitrinite Reflectance ($R_{o,max}$ %) & Temperature (T °C)

The Graphs between Langmuir Pressure constant (P_L) and different variables have been plotted with varying only one variable while keeping other variables constant. The Graphs between Langmuir Pressure constant (P_L) Vs Moisture on air dry basis in % (M_{ad} %) (Fig. 8a₁), Fixed Carbon (FC_{ad} %) to Moisture (M_{ad} %) ratio on air dry basis (Fig. 8a₂), Volatile Matter on air dry basis in % (VM_{ad} %) (Fig. 8b₁), Volatile Matter (VM_{ad} %) ratio on air dry basis (Fig. 8b₂), Ash on air dry basis in % (A_{ad} %) (Fig. 8c₁), Fixed Carbon (FC_{ad} %) to Ash (A_{ad} %) ratio on air dry basis (Fig. 8c₂), Vitrinite Reflectance ($R_{o,max}$ %) (Fig. 8d) & Temperature (T °C) (Fig. 8e) have been plotted, which are respectively shown below:

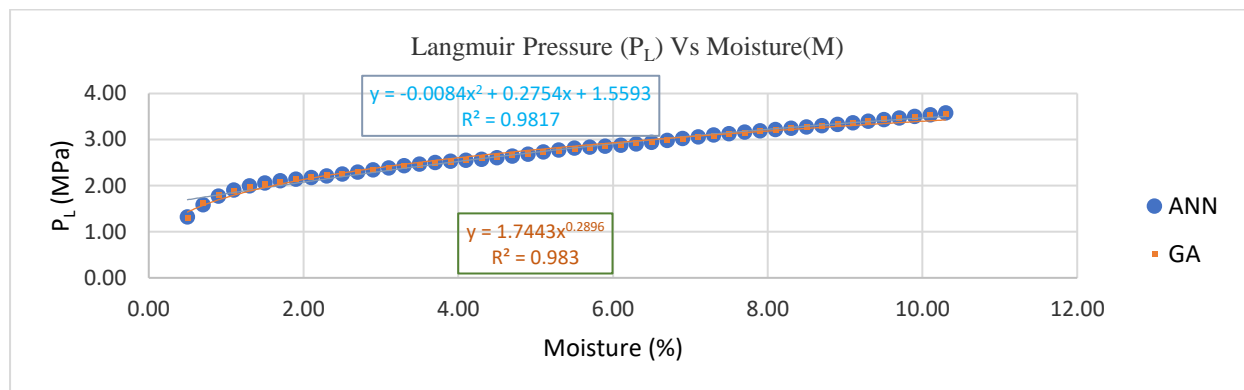


Fig. 8a₁ (Langmuir Pressure (P_L) Vs Moisture(M))

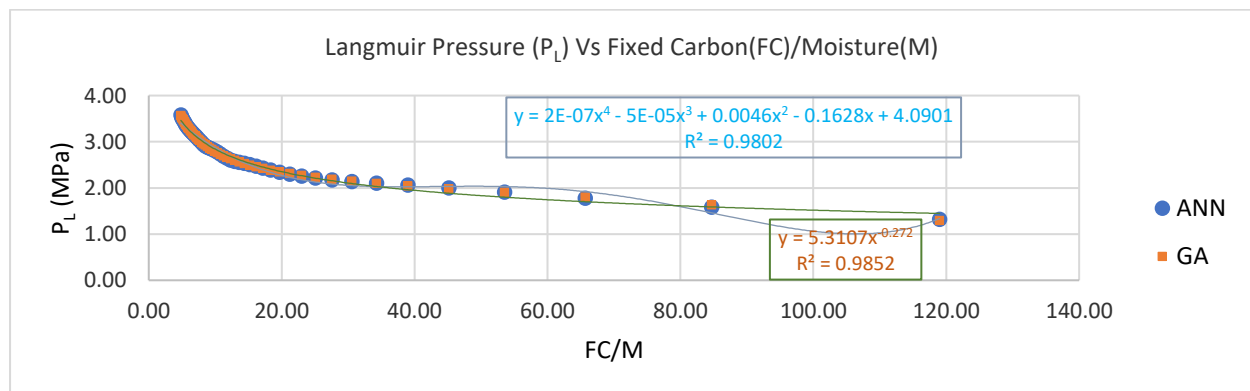
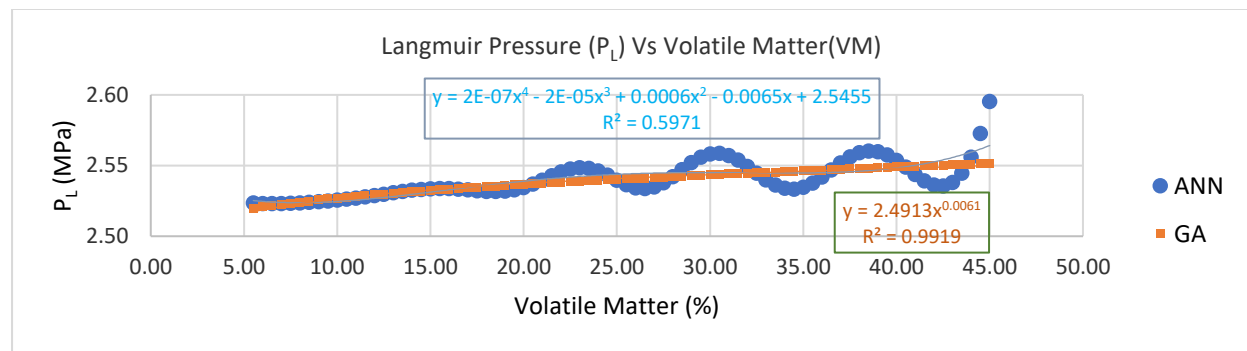
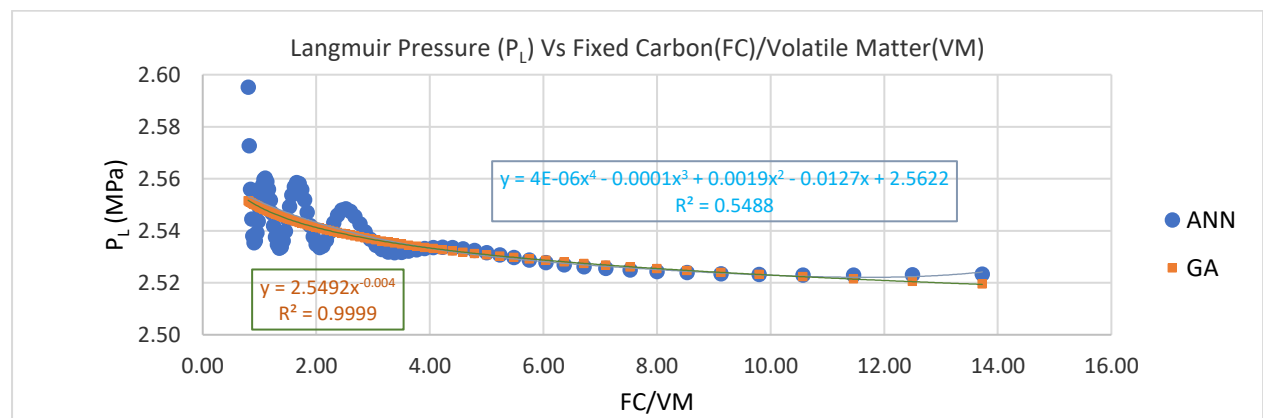
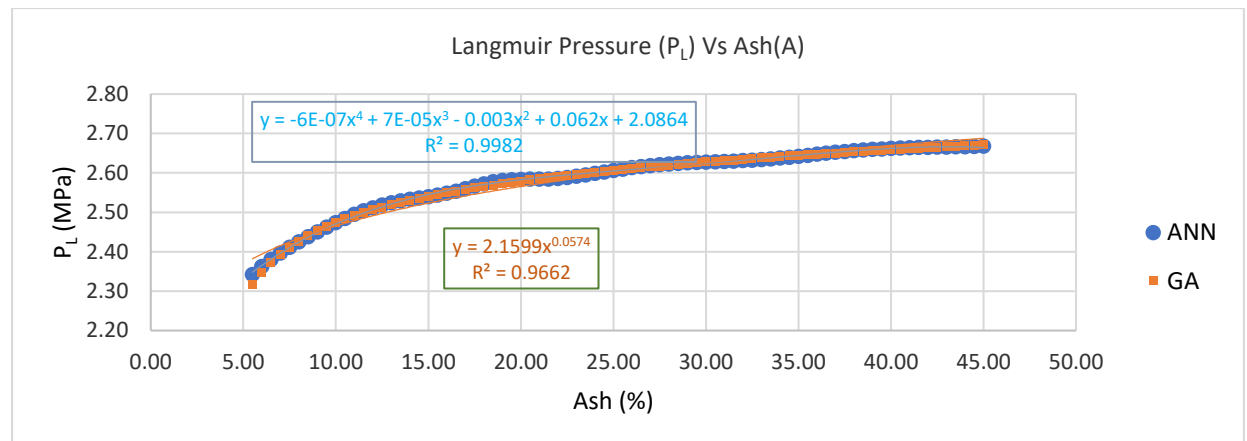
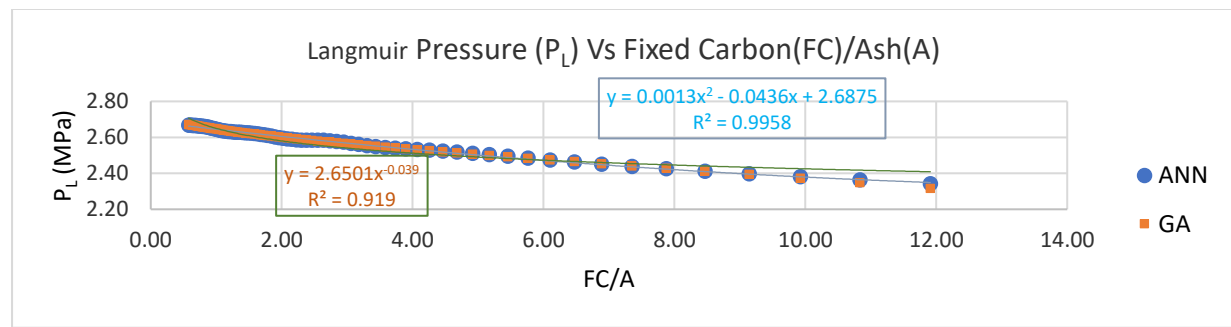
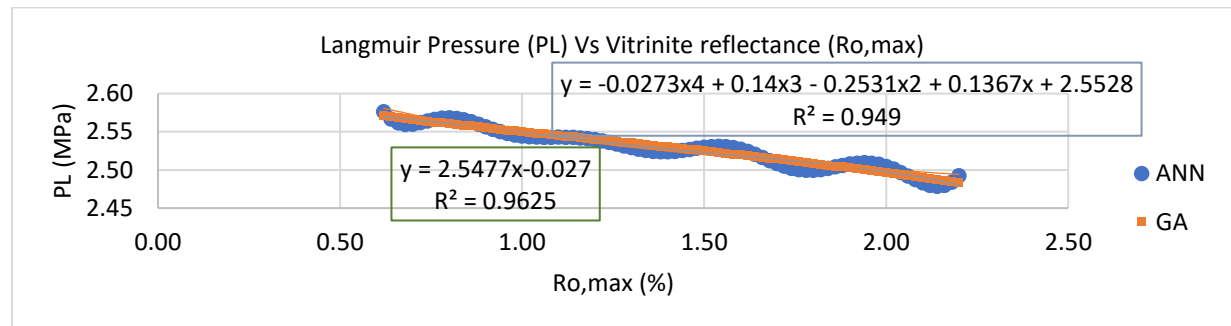
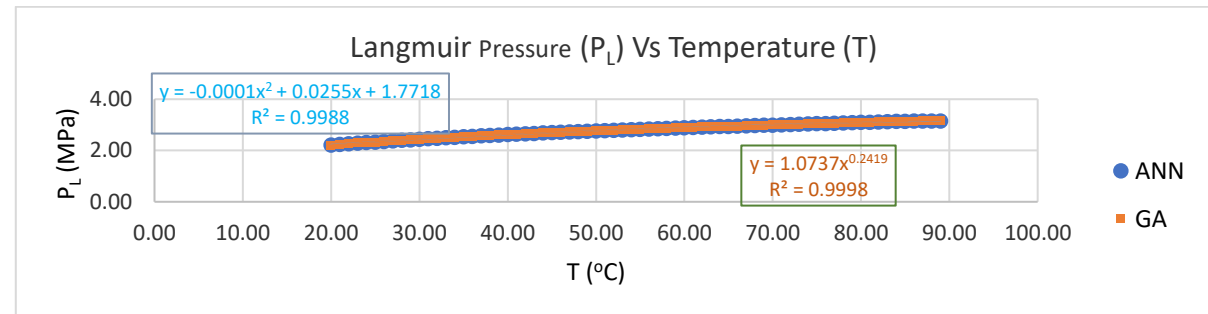


Fig. 8(a2) (Langmuir Pressure (P_L) Vs Fixed Carbon (FC)/Moisture (M))

Fig. 8 b₁ (Langmuir Pressure (P_L) Vs Volatile Matter (VM))Fig. 8b₂ (Langmuir Pressure (P_L) Vs Fixed Carbon (FC)/Volatile Matter (VM))Fig. 8c₁ (Langmuir Pressure (P_L) Vs Ash (A))

Fig. 8c₂ (Langmuir Pressure (P_L) Vs Fixed Carbon(FC)/Ash(A))Fig. 8d (Langmuir Pressure (P_L) Vs Vitrinite reflectance ($R_{o,max}$))Fig. 8e (Langmuir Pressure (P_L) Vs Temperature (T))

The different plotted graph as per both GA & ANN prediction model reveal that

- as Moisture (M_{ad} %) increases Langmuir Pressure constant (P_L) value gradually increases (Fig. 8a₁),
- as ratio of Fixed carbon (FC_{ad} %) to Moisture (M_{ad} %) increases Langmuir Pressure constant (P_L) value decreases (Fig. 8a₂),
- as Volatile Matter (VM_{ad} %) increases Langmuir Pressure constant (P_L) value increases (Fig. 8b₁),
- as ratio of Fixed carbon (FC_{ad} %) to Moisture (M_{ad} %) increases Langmuir Pressure constant (P_L) value decrease (Fig. 8b₂),
- as Ash (A_{ad} %) increases Langmuir Pressure constant (P_L) value increase (Fig. 8c₁),
- as ratio of Fixed carbon (FC_{ad} %) to Ash (A_{ad} %) increases Langmuir Pressure constant (P_L) value decrease (Fig. 8c₂),
- as Vitrinite Reflectance ($R_{o,max}$ %) increases Langmuir Pressure constant (P_L) value decreases (Fig. 8d),
- as Temperature (T °C) increases Langmuir Pressure constant (P_L) value increases (Fig. 8e).

Langmuir Volume Constant (V_L) Vs Moisture (M_{ad} %), Volatile Matter (VM_{ad} %), Ash (A_{ad} %), Vitrinite Reflectance ($R_{o,max}$ %) & Temperature (T °C)

The Graphs between Langmuir Volume constant (V_L) and different variables have been plotted with varying only one variable while keeping other variables constant. The Graphs between Langmuir Volume constant (V_L) Vs Moisture on air dry basis in % (M_{ad} %) (Fig. 9a₁), Fixed Carbon (FC_{ad} %) to Moisture (M_{ad} %) ratio on air dry basis (Fig. 9a₂), Volatile Matter on air dry basis in % (VM_{ad} %) (Fig. 9b₁), Volatile Matter (VM_{ad} %) ratio on air dry basis (Fig. 9b₂), Ash on air dry basis in % (A_{ad} %) (Fig. 9c₁), Fixed Carbon (FC_{ad} %) to Ash (A_{ad} %) ratio on air dry basis (Fig. 9c₂), Vitrinite Reflectance ($R_{o,max}$ %) (Fig. 9d) & Temperature (T °C) (Fig. 9e) have been plotted, which are respectively shown below:

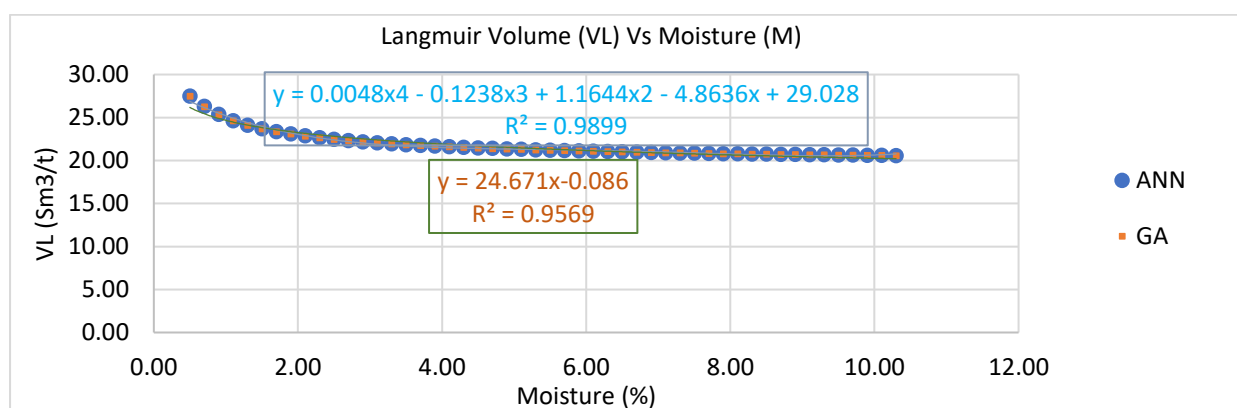


Fig. 9a₁ (Langmuir Volume (V_L) Vs Moisture (M))

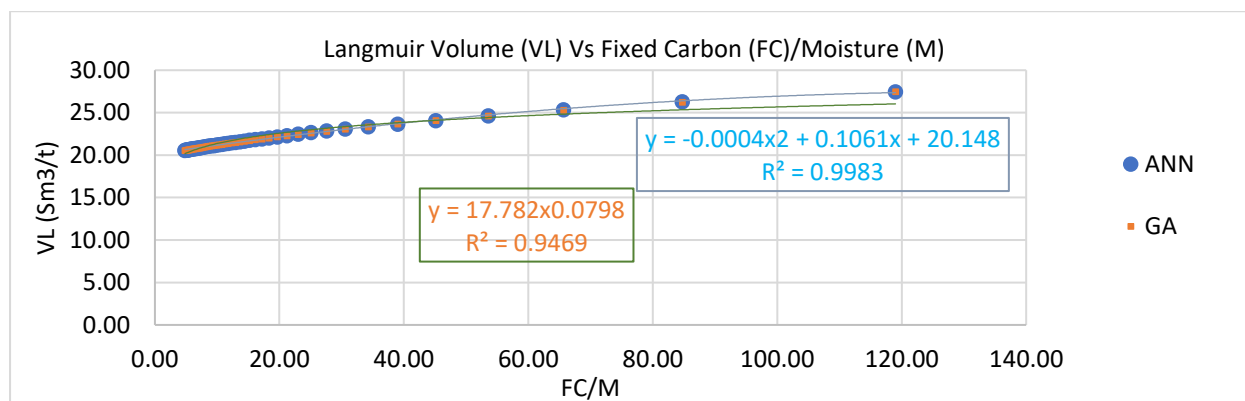


Fig. 9a₂ (Langmuir Volume (V_L) Vs Fixed Carbon (FC)/Moisture (M))

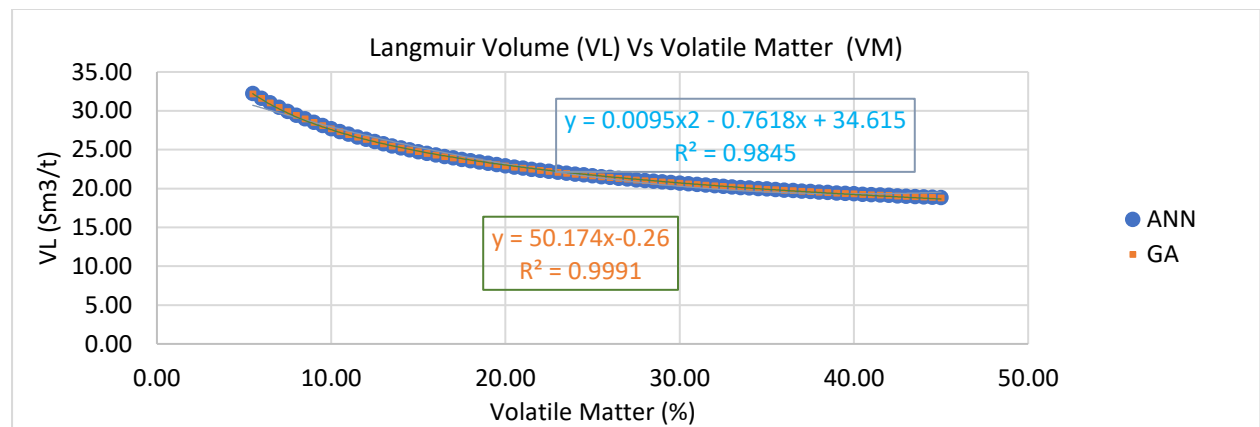


Fig. 9b₁ (Langmuir Volume (VL) Vs Volatile Matter (VM))

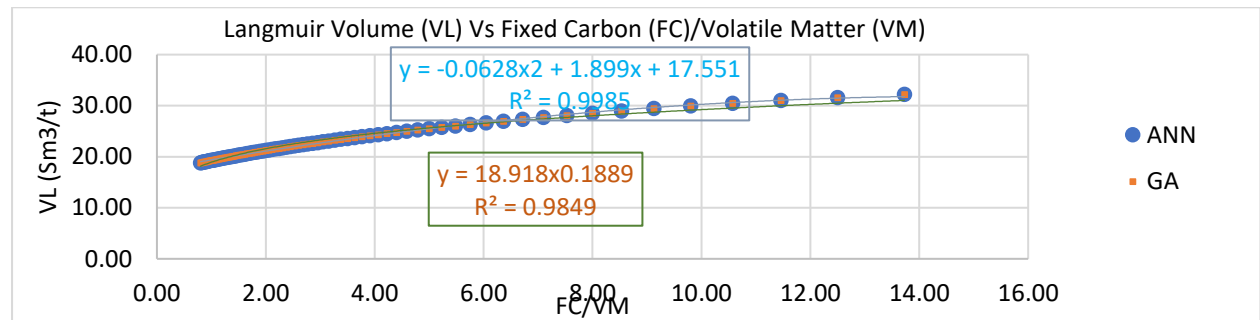


Fig. 9b₂ (Langmuir Volume (VL) Vs Fixed Carbon (FC)/Volatile Matter (VM))

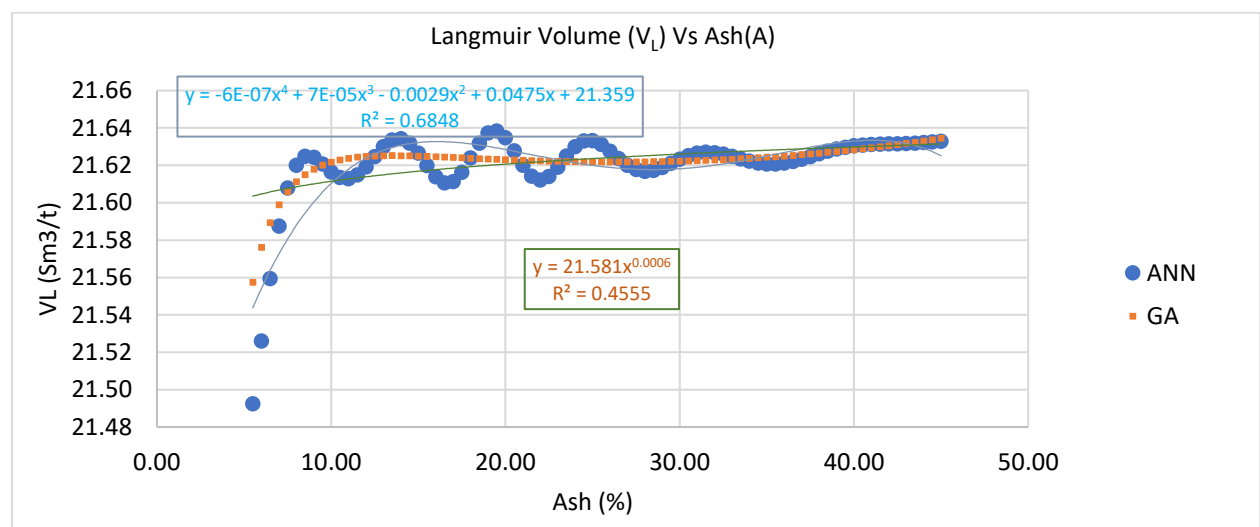
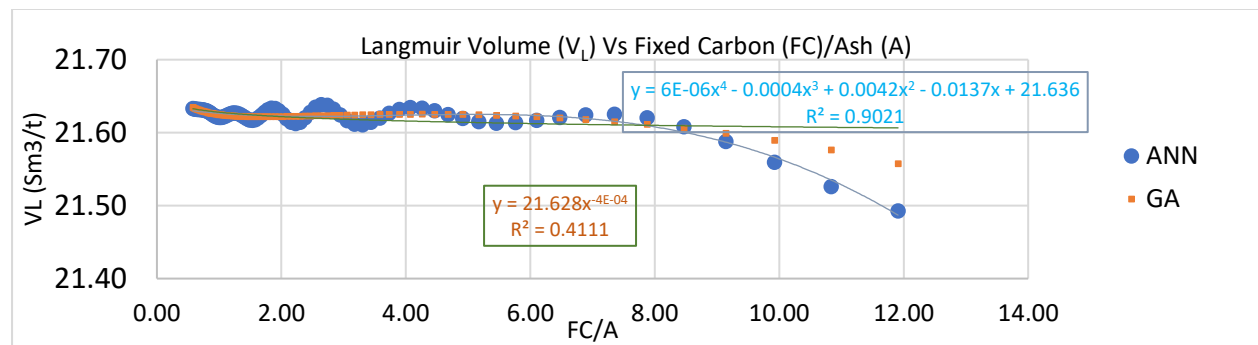
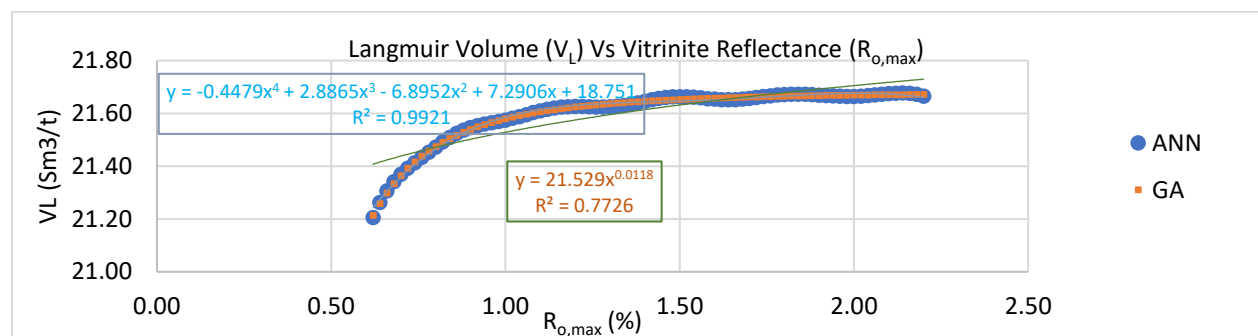
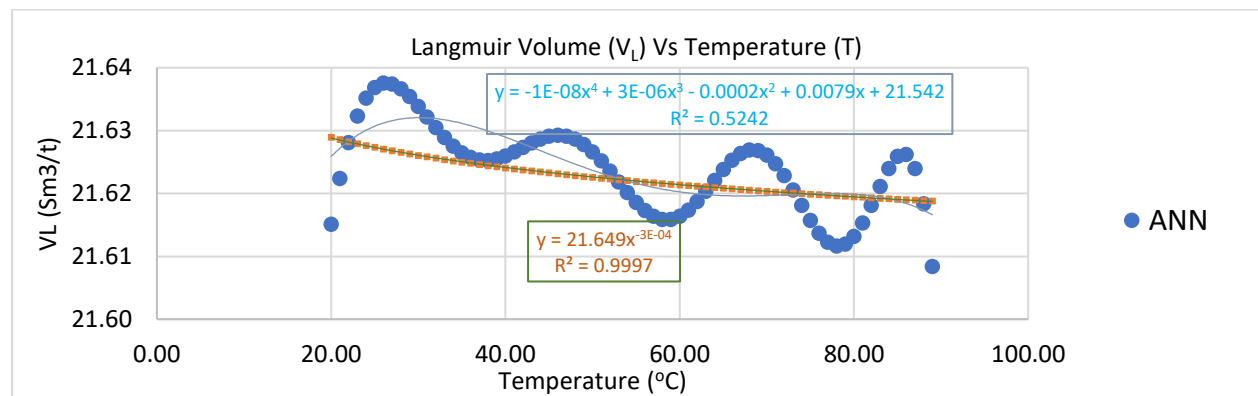


Fig. 9c₁ (Langmuir Volume (VL) Vs Ash(A))

Fig. 9c₂ (Langmuir Volume (V_L) Vs Fixed Carbon (FC)/Ash (A))Fig. 9d (Langmuir Volume (V_L) Vs Vitrinite Reflectance ($R_{o,max}$))Fig. 9e (Langmuir Volume (V_L) Vs Temperature (T))

The different plotted graph as per both GA & ANN prediction model reveal that

- as Moisture (M_{ad} %) increases Langmuir Volume constant (V_L) value slightly decreases (Fig. 9a₁),
- as ratio of Fixed carbon (FC_{ad} %) to Moisture (M_{ad} %) increases Langmuir Volume constant (V_L) value increases (Fig. 9a₂),
- as Volatile Matter (VM_{ad} %) increases Langmuir Volume constant (V_L) value decreases (Fig. 9b₁),
- as ratio of Fixed carbon (FC_{ad} %) to Moisture (M_{ad} %) increases Langmuir Volume constant (V_L) value increases (Fig. 9b₂),
- as Ash (A_{ad} %) increases Langmuir Volume constant (V_L) value is mostly constant (Fig. 9c₁),
- as ratio of Fixed carbon (FC_{ad} %) to Ash (A_{ad} %) increases Langmuir Volume constant (V_L) value is mostly constant (Fig. 9c₂),
- as Vitrinite Reflectance ($R_{o,max}$ %) increases Langmuir Volume constant (V_L) value increases (Fig. 9d),

- as Temperature (T °C) increases Langmuir Volume constant (V_L) value is almost constant (Fig. 9e). So, Langmuir Volume constant (V_L) is temperature independent.

Above plotted different graphs shows that Langmuir Pressure constant (P_L) increases as Moisture (M_{ad} %), Volatile Matter (VM_{ad} %), Ash (A_{ad} %) & Temperature (T °C) increases, while P_L decreases as Vitrinite Reflectance ($R_{o,max}$ %) increases. Langmuir Volume constant (V_L) increases as Vitrinite Reflectance ($R_{o,max}$ %) increases, while V_L decreases as Moisture (M_{ad} %) & Volatile Matter (VM_{ad} %) increases. Langmuir Volume constant (V_L) is independent from Temperature (T °C). So it can be concluded that Langmuir Volume Constant (V_L) depends on properties of sorbent only while Langmuir Pressure constant (P_L) depends on properties of sorbent and physical condition of sorption system.

5. Discussion

This study shows that GA prediction model and GA-ANN prediction model both are predicting the Langmuir constants (P_L & V_L) with greater level of accuracy than other earlier provided prediction model. GA-ANN prediction model least error in prediction. So GA-ANN model can be used for prediction with greater level of accuracy and confidence.

The correlation study of Langmuir constants with influencing parameters revealed the behavioral dependency of Langmuir constants on influencing parameters. Langmuir Pressure constant (P_L) is increases as temperature increases while Langmuir Volume Constant (V_L) is independent of temperature. Langmuir Constant P_L depends on coal quality parameters (sorbent properties) as well as temperature (physical condition of sorption system) both while Langmuir Constant V_L depends only on coal quality parameters (sorbent properties) and independent of temperature (physical condition of sorption system). Moisture and Ash content have negative impact on sorption of gas.

References

- [1] R. E. Rogers, *Coalbed-methane-principles-and-practices.pdf*, Second. Halliburton: Oktibbeha Publishing Co. LLC, Starkville, MS 39759, 1994.
- [2] A. Boruah, B. Kumar, H. Rao P, and T. Harinarayana, "Integrated Development Of Both Conventional And Unconventional Coal Fuels In India," *The International Journal Of Science & Technoledge*, vol. 5, pp. 11–17, 2013.
- [3] Z. Di Liu, J. Z. Zhao, P. Zhang, and J. X. Sun, "Evaluating the CBM reservoirs using NMR logging data," *Open Geosci.*, vol. 10, no. 1, pp. 544–553, 2018, doi: 10.1515/geo-2018-0043.
- [4] D. Hao *et al.*, "Experimental study of the moisture content influence on CH₄ adsorption and deformation characteristics of cylindrical bituminous coal core," *Adsorpt. Sci. Technol.*, vol. 36, no. 7–8, pp. 1512–1537, 2018, doi: 10.1177/0263617418788444.
- [5] J. Zhang, L. Si, J. Chen, M. Kizil, C. Wang, and Z. Chen, "Stimulation Techniques of Coalbed Methane Reservoirs," *Geofluids*, vol. 2020, 2020, doi: 10.1155/2020/5152646.
- [6] W. Chao, "Coalbed methane reservoir characteristics and well logging evaluation method," vol. 06, no. 03, pp. 51–54, 2016.
- [7] A. Keshavarz, R. Sakurovs, M. Grigore, and M. Sayyafzadeh, "Effect of maceral composition and coal rank on gas diffusion in Australian coals," *Int. J. Coal Geol.*, vol. 173, pp. 65–75, 2017, doi: 10.1016/j.coal.2017.02.005.
- [8] T. Cai, Z. Feng, Y. Jiang, and D. Zhao, "Thermodynamic Characteristics of Methane Adsorption of Coal with Different Initial Gas Pressures at Different Temperatures," *Adv. Mater. Sci. Eng.*, vol. 2019, p. 9, 2019, doi: 10.1155/2019/4751209.
- [9] S. Singh, A. Boruah, and J. Devaraju, "CO₂ sequestration and CH₄ extraction from unmineable coal seams in Singrauli coalfield," *International Journal of Coal Preparation and Utilization*. 2023. doi:

- 10.1080/19392699.2023.2280134.
- [10] M. A. Rasheed *et al.*, “Geochemical Characterization of Coals Using Proximate and Ultimate Analysis of Tadkeshwar Coals, Gujarat,” *Geosciences*, vol. 2015, no. 4, pp. 113–119, 2015. [Online]. Available: <http://journal.sapub.org/geo>
 - [11] L. Zhang, N. Aziz, T. Ren, and Z. Wang, “Influence of Temperature on the Gas Content of Coal and Sorption Modelling,” in *11th Underground Coal Operators’ Conference, University of Wollongong & the Australasian Institute of Mining and Metallurgy*, 2011, pp. 269–276. [Online]. Available: research-pubs@uow.edu.au
 - [12] A. K. Verma and A. Sirvaiya, “Intelligent prediction of Langmuir isotherms of Gondwana coals in India,” *J. Pet. Explor. Prod. Technol.*, vol. 6, no. 1, pp. 135–143, 2016, doi: 10.1007/s13202-015-0157-y.
 - [13] X. Tang and N. Ripepi, “Temperature-dependent Langmuir’s model in the coal and methane sorption process: Statistics relationship,” *2016 SME Annu. Conf. Expo Futur. Min. a Data-Driven World*, no. January, pp. 242–249, 2016, doi: 10.19150/trans.7328.
 - [14] Z. Li and X. Hu, “Measurement of gas diffusion coefficient and analysis of influencing factors for Shaanxi Debao coalbed methane reservoir in China,” *J. Pet. Explor. Prod. Technol.*, vol. 11, no. 2, pp. 735–746, 2021, doi: 10.1007/s13202-020-01058-1.
 - [15] J. Huang, S. Liu, S. Tang, S. Shi, and C. Wang, “Study on the coalbed methane development under high in situ stress, large buried depth, and low permeability reservoir in the Libi block, Qinshui Basin, China,” *Adv. Civ. Eng.*, vol. 2020, 2020, doi: 10.1155/2020/6663496.
 - [16] P. Dutta, S. Harpalani, and B. Prusty, “Modeling of CO₂ sorption on coal,” *Fuel*, vol. 87, no. 10–11, pp. 2023–2036, 2008, doi: 10.1016/j.fuel.2007.12.015.
 - [17] G.-M. Schwab, “Physical Chemistry, Von F. Daniels und R. A. Alberty. John Wiley and Sons, Inc. New York. 1955. 1. Aufl. VIII, 671 S., gebd. \$ 6.50,” *Angew. Chemie*, vol. 68, no. 7, pp. 252–252, Apr. 1956, doi: 10.1002/ange.19560680714.
 - [18] B. Adiraju, “Adsorption of CO₂ on Indian coals,” National Institute of Technology, Rourkela-769008, Orissa, India, 2010. [Online]. Available: [http://ethesis.nitrkl.ac.in/2026/1/Bharadwaj\(208CH103\).pdf](http://ethesis.nitrkl.ac.in/2026/1/Bharadwaj(208CH103).pdf)
 - [19] J. M. Hawkins, R. Houston, R. A. Schraufnagel, A. J. Olszewski, and R. Pittsburgh, “Estimating Coalbed Gas Content and Sorption Isotherm Using Well Log Data,” in *Annual Technical Conference and Exhibition of the Society of Petroleum Engineers*, 1992, no. 67th, p. SPE-24905-MS. doi: <https://doi.org/10.2118/24905-MS>.
 - [20] J. Shen, Y. Qin, X. Fu, G. Wang, R. Chen, and L. Zhao, “Study of high-pressure sorption of methane on Chinese coals of different rank,” *Arab. J. Geosci.*, vol. 8, no. 6, pp. 3451–3460, 2015, doi: 10.1007/s12517-014-1459-y.
 - [21] A. G. Kim, “Estimating Methane Content of Bituminous Coalbeds From Adsorption Data.,” *US Bur Mines Rep Invest*, no. 8245, 1977.
 - [22] N. Radhika, P. Shivaram, and K. T. Vijay Karthik, “Multi-objective optimization in electric discharge machining of aluminium composite,” *Tribol. Ind.*, vol. 36, no. 4, pp. 428–436, 2014.
 - [23] G. F. Luger, “A Brief History of the Foundations for AL,” *Artif. Intell.*, p. 5, 2005.
 - [24] M. Fridrich, “Hyperparameter Optimization of Artificial Neural Network in Customer Churn Prediction using Genetic Algorithm,” *Trends Econ. Manag.*, vol. 28, no. 1, pp. 9–21, 2017, [Online]. Available: <https://search-proquest-com.aib.idm.oclc.org/docview/1912541562/fulltextPDF/74E19B402184475BPQ>
 - [25] P. G. Benardos and G. C. Vosniakos, “Optimizing feedforward artificial neural network architecture,”

- Eng. Appl. Artif. Intell.*, vol. 20, no. 3, pp. 365–382, 2007, doi: 10.1016/j.engappai.2006.06.005.
- [26] F. Giannini, V. Laveglia, A. Rossi, D. Zanca, and A. Zugarini, “Neural Networks for Beginners. A fast implementation in Matlab, Torch, TensorFlow,” pp. 1–48, 2017, [Online]. Available: <http://arxiv.org/abs/1703.05298>
- [27] Md. Mijanur Rahman and ania Akter Setu, “An Implementation for Combining Neural Networks and Genetic Algorithms,” *Int. J. Comput. Sci. Technol.*, vol. 6, no. 3, pp. 218–222, 2015.
- [28] X. Li, X. Yan, and Y. Kang, “Effect of temperature on the permeability of gas adsorbed coal under triaxial stress conditions,” *J. Geophys. Eng.*, vol. 15, no. 2, pp. 386–396, 2018, doi: 10.1088/1742-2140/aa9a98.
- [29] R. Pini, “Research Collection,” *Brisk Bin. Robust Invariant Scalable Keypoints*, pp. 12–19, 2009, doi: 10.3929/ethz-a-010782581.
- [30] A. M. Pophare, V. A. Mendhe, and A. Varade, “Evaluation of coal bed methane potential of coal seams of Sawang Colliery, Jharkhand, India,” *J. Earth Syst. Sci.*, vol. 117, no. 2, pp. 121–132, 2008, doi: 10.1007/s12040-008-0003-4.
- [31] P. Dutta, S. Bhowmik, and S. Das, “Methane and carbon dioxide sorption on a set of coals from India,” *Int. J. Coal Geol.*, vol. 85, no. 3–4, pp. 289–299, 2011, doi: 10.1016/j.coal.2010.12.004.

Annexure-I

Sl. No.	Experimentally Measured Data Set on Air dry basis (ad)								Location of considered Coal Sample	Literature Reference
	Moisture (%) (ad)	Volatile Matter (%) (ad)	Fixed Carbon (%) (ad)	Ash (%) (ad)	R _{o,max} (%)	Temperature (°C)	Measured Langmuir Constt. for CH ₄			
							Pressure Constt. (P _L) (Mpa)	Volume Constt. (V _L) (sm ³ /t) daf		
1	10.00	31.10	45.60	13.30	1.04	36	3.01	19.66	Main Basin of Singrauli Coal Filed, India	Experimental Data Set estimate by Researcher
2	4.70	19.90	25.70	49.70	1.57	37	2.11	22.41		
3	7.10	30.70	47.00	15.20	1.06	38	2.67	19.90		
4	8.40	30.10	42.80	18.70	1.08	39	3.16	20.38		
5	8.00	29.20	45.60	17.20	1.12	39	2.98	20.28		
6	6.83	31.13	40.40	21.63	1.04	34	2.54	19.88		
7	6.78	20.53	59.86	12.84	1.53	35	2.80	22.74		
8	3.90	27.30	34.00	34.80	1.20	35	2.12	21.35		
9	6.70	27.30	47.50	18.50	1.20	37	3.03	21.43		
10	7.33	29.69	40.04	22.95	1.10	37	2.50	19.25		
11	6.35	37.32	41.86	14.48	0.83	33	2.80	19.92		
12	7.04	41.17	17.69	34.10	0.71	34	2.77	18.77		
13	7.12	26.23	37.19	29.47	1.24	34	2.85	21.48		
14	5.70	21.90	35.90	36.50	1.46	34	2.63	22.89		
15	3.73	40.76	19.19	36.33	0.72	34	1.86	18.25		
16	6.20	14.26	49.91	29.63	1.96	34	2.95	26.01		
17	7.17	31.11	39.07	22.65	1.04	35	2.51	19.55		
18	7.10	15.04	55.19	22.68	1.90	35	2.79	24.27		
19	7.00	28.50	42.60	21.90	1.15	37	3.12	21.58		
20	12.70	26.57	40.04	20.69	1.23	37	3.51	20.60		

21	1.28	34.32	55.52	8.88	1.02	30	3.01	15.46	Shanxi, China	[28]
22	1.05	11.82	76.99	10.14	2.26	20	0.36	20.66	Gucheng, China	[8]
23	1.05	11.82	76.99	10.14	2.26	30	0.36	20.37		
24	1.05	11.82	76.99	10.14	2.26	40	0.36	20.04		
25	1.05	11.82	76.99	10.14	2.26	50	0.35	19.65		
26	1.05	11.82	76.99	10.14	2.26	60	0.34	19.08		
27	1.05	11.82	76.99	10.14	2.26	70	0.34	18.80		
28	1.05	11.82	76.99	10.14	2.26	80	0.34	18.48		
29	1.05	11.82	76.99	10.14	2.26	90	0.34	18.05		
30	1.08	14.02	76.21	8.69	2.02	20	0.31	21.51		
31	1.08	14.02	76.21	8.69	2.02	30	0.31	21.23	Gaohe, China	
32	1.08	14.02	76.21	8.69	2.02	40	0.31	20.92		
33	1.08	14.02	76.21	8.69	2.02	50	0.31	20.70		
34	1.08	14.02	76.21	8.69	2.02	60	0.30	20.33		
35	1.08	14.02	76.21	8.69	2.02	70	0.30	20.04		
36	1.08	14.02	76.21	8.69	2.02	80	0.30	19.84		
37	1.08	14.02	76.21	8.69	2.02	90	0.30	19.61		
38	8.10	40.31	46.39	5.20	0.57	30	9.14	17.89	Yangpoqua m, China	
39	8.10	40.31	46.39	5.20	0.57	50	11.00	15.34		
40	8.10	40.31	46.39	5.20	0.57	70	10.05	11.10		
41	7.20	30.46	51.94	10.40	0.84	30	7.42	23.09	Wangtian, China	
42	7.20	30.46	51.94	10.40	0.84	50	9.47	23.04		
43	7.20	30.46	51.94	10.40	0.84	70	9.89	14.81		
44	6.40	22.96	59.24	11.40	1.17	30	5.15	22.47	Nanyu, China	[20]
45	6.40	22.96	59.24	11.40	1.17	50	4.61	18.76		
46	6.40	22.96	59.24	11.40	1.17	70	4.66	15.60		
47	2.90	16.57	67.43	13.10	1.58	30	4.48	23.64	Shungliu, China	
48	2.90	16.57	67.43	13.10	1.58	50	4.97	22.12		
49	2.90	16.57	67.43	13.10	1.58	70	4.33	13.62		
50	4.20	5.34	75.66	14.80	2.87	30	4.41	46.95	Chengzhuan g, China	
51	4.20	5.34	75.66	14.80	2.87	50	5.26	45.45		
52	4.20	5.34	75.66	14.80	2.87	70	9.81	48.54		
53	7.80	30.99	50.09	11.12	0.74	45	2.67	39.65	Itly	
54	7.80	30.99	50.09	11.12	0.74	33	2.10	40.54		
55	7.80	30.99	50.09	11.12	0.74	60	3.18	37.41		
56	5.32	40.25	45.72	8.71	0.7	45	1.71	36.51		
57	1.00	28.8	53.50	16.70	0.85	45	2.91	33.15	Switezeland	[29]
58	0.80	26.7	44.20	28.30	0.90	45	3.22	28.00		
59	1.63	25.29	56.12	12.66	0.80	55	2.39	25.31	Australia	
60	1.63	25.29	56.12	12.66	0.80	45	2.20	25.98		
61	0.39	17.65	64.16	17.80	1.34	45	2.81	40.32		

62	2.98	28.31	55.93	12.78	1.15	30	2.86	24.94	Jharia, India	[30]
63	2.01	27.72	50.60	19.67	1.18	30	3.75	26.88		
64	2.61	33.86	52.61	10.92	0.94	30	2.49	22.99		
65	1.45	27.01	41.53	30.01	1.21	30	2.92	22.94		
66	1.28	29.34	51.12	18.26	1.11	30	2.70	23.36		
67	7.00	38.00	45.00	10.00	0.64	30	2.70	33.00	Jharia, India	[31]
68	4.00	40.00	44.00	12.00	0.62	30	3.08	24.00		
69	7.00	41.00	37.00	15.00	0.64	30	7.35	36.00		
70	4.00	40.00	39.00	17.00	0.61	30	2.55	23.00		
71	1.20	36.00	34.80	28.00	0.96	30	1.89	16.00		
72	2.30	41.50	34.20	22.00	1.01	30	1.32	12.00		
73	1.10	35.00	33.90	30.00	0.96	30	3.61	23.00		
74	2.20	38.00	32.80	27.00	1.06	30	1.85	13.00		
75	1.40	34.00	33.60	31.00	1.94	30	1.10	22.00		
76	1.80	32.00	18.20	48.00	1.30	30	1.06	22.00		
77	1.20	45.00	33.80	20.00	1.29	30	2.03	24.00		
78	1.60	36.50	37.90	24.00	1.22	30	1.82	27.00		
79	6.00	35.00	25.00	34.00	1.11	30	2.41	28.00		
80	0.50	38.00	39.50	22.00	0.97	30	1.75	22.00		